Short-Range-Ordering of Deuterium in α -TaD0.55

Materials Transactions, JIM, Vol. 32, No. 7 (1991), pp. 567 to 573

Short-Range-Ordering of Deuterium in α-$TaD_{0.55}$

H. Kaneko*†, T. Kajitani*, M. Hirabayashi*†† and M. Sakamoto**

Elastic neutron scattering technique has been employed to study the short-range-ordering of deuterium atoms in α-$TaD_{0.55}$ in the temperature range 65–80°C. The intensity distribution of 1/2 1/2 0 type diffuse pseudo-Bragg reflections is observed. Intensities of the 1/2 1/2 0 type diffuse reflection are not much temperature dependent as in the case of those observed in α-$VD_{0.5}$ and α-NbH_x=0.05−0.6. Warren-Cowley's short range order parameter and the short range displacement are calculated.

The existence of almost spherical microdomains having a β_2-$TaD_{0.5}$-type structure with a diameter of about 1.2 nm is concluded from the present neutron diffraction work.

(Received March 18, 1991)

Keywords: *neutron scattering, tantalum deuteride, deuterium, diffuse scattering, short range order, displacement, Huang scattering*

I. Introduction

Hydrogen-isotopes are easily dissolved in the group V_a metals (V, Nb and Ta) up to the hydrogen concentration vs metal ratio about 1.0 at moderate temperatures below 200°C. Hydrogen-isotopes are mainly situated at the tetrahedral interstices. The term "lattice gas" has been used to describe hydrogen isotopes in α-phases of the group V_a metals plus hydrogen-isotope systems. However, hydrogen-isotopes have been found not to be thoroughly free in metal lattices. Each hydrogen-isotope atom blocks another hydrogen-isotope atom to sit in the range from the first to the third nearest tetrahedral interstices[1][2]. Diffuse halo-like reflections due to the blocking effect has been observed in powder neutron diffraction spectra by Somenkov and Shill'stein[3]. At the same time, isolated but diffuse Bragg-like reflections have been also found between the fundamental reflections. Jo and Moss[4] and Burkel *et al.*[5] reported weakly temperature-dependent isolated X-ray diffuse reflections at 1/2 1/2 0 and its equivalent wave numbers in α-$VD_{0.5}$ and α-NbH_x (x=0.05-0.6), respectively. Isolated diffuse-reflections were interpreted in terms of structural fluctuations and microdomains which have a similar ordered structure of the low temperature phases, i.e. β-$VD_{0.5}$ or ζ-NbH_x (x=0.5), respectively. The domain size was estimated at about 1.0 to 2.0 nm from the FWHM of the diffuse reflections in α-$VD_{0.5}$[4]. Brun *et al.*[6] and Shasnov[7] observed asymmetric Huang scatterings in the vicinities of Bragg reflections in α-$NbD_{0.8}$ (Brun *et al.*) by the neutron diffraction and α-NbH_x and α-NbD_x ($0.70<x<0.85$) (Shasnov) by X-ray and neutron diffractions. It has been implied that the Huang scatterings are originated from a kind of precipitates or microdomains which introduce some distortion of the matrix. Asymmetric nature of the Huang scatterings indicates that such microdomains are surrounded by a strain field[8] which is accommodated in a finite volume. Magerl *et al.*[9] reported continuous shift of neutron inelastic scattering peaks due to hydrogen local vibration modes in α-$NbH_{0.005}$ and α-TaH_x (x=0.037, 0.18) as a function of temperature from 78 to 295 K and of hydrogen concentration, respectively. The cause of the shift has been discussed in terms of the hydrogen concentration fluctuation, ordered microdomains and tunneling of hydrogen atoms. Watanabe and Fukai[10] carefully measured the entropy changes due to $\beta_1-\beta_2$ and $\beta_2-\alpha$ phase transformations in $V_{1-y}M_yH_x$ ($0.5<x<0.6$, M=Mo, Fe, Cr, Nb, Ti, Zr, $Y<0.02$) as a function of hydrogen concentration and the effect of alloying. Entropy change by the $\beta_1-\beta_2$ transformation ΔS ($\beta_1\rightarrow\beta_2$) changed strongly by the substitution of M for V whereas the entropy change ΔS($\beta_1\rightarrow\alpha$) was little affected. The change was interpreted with the presence of short-range ordering in the α- and β_2-phases. Watanabe *et al.* estimated the local correlations of hydrogen (deuterium) atoms in α-$VH(D)_x$ ($x\sim0.5$) extend to three or four hydrogen (deuterium) atoms which are blocked each other. Efforts were focussed to determine the short-range order-parameter and short-range displacement in the microdomains in α-$TaD_{0.55}$ at 65°C out of neutron diffuse scattering intensities.

II. Diffraction Theory

Following Borie and Sparks[11][12], the diffraction intensities from such inhomogeneous systems have been approximated from kinematical theory:

$$I=\sum_p\sum_q f_pf_q\exp[ik(R_p-R_q)]+i\sum_p\sum_q f_pf_qk(\delta_p-\delta_q)\times\exp[ik(R_p-R_q)]-1/2\sum_p\sum_q f_pf_q[k(\delta_p\delta_q)]^2\times\exp[ik(R_p-R_q)], \quad (1)$$

* The Institute for Materials Research, Tohoku University, Sendai 980, Japan.
† Present address: Research and Development Center, Toshiba Co., Kawasaki 210, Japan.
†† Present address: Kitami Institute of Technology, Kitami, Hokkaido 090, Japan.
** Department of Physics, Japan Atomic Energy Research Institute, Tokai, Ibaragi 319-11, Japan.

where f_p is an atomic scattering factor for X-ray diffraction or an atomic scattering length for neutron diffraction, respectively. The p-th atom is supposed to site nearly but not exactly at the site R_p of a periodic structure. The deviation δ_p from the exact position R_p enters in the second term. The first term is the intensity due to a chemical atomic arrangement without displacements from ideal atomic sites. The second term which was discovered by Warren *et al.*[13] originated from the displacement or modulation of a lattice. The second term was originally referred as the atomic size effect term[13][14] in the case of short range ordered substitutional systems. This term gives strong diffuse intensities in the higher wave number regions. The third term is the intensity of Huang (+Trinkaus) scattering[8][15][16].

The first term found by Cowley[17] consists of the sharp Bragg reflection and a diffuse intensity which is also a summation of the monotonic back ground intensity and a three-dimensional Fourier series of local atomic arrangements.

In a case of binary substitutional systems, the first term becomes

$$I_1/Nf_A^2=(m_A+m_B\eta)^2/N\sum_p\sum_q \exp\,[ik(R_p-R_q)] + m_Am_B(1-\eta)^2\sum_q \alpha_{pq}\exp\,[ik(R_p-R_q)], \quad (2)$$

where the two kinds of atoms A and B are identified by subscripts. m_A and m_B are the fractions of the total number of atoms N. η is the ratio f_A/f_B. α_{pq} is the Warren-Cowley's (chemical) short-range order-parameter.

The first term in eq. (2) corresponds to the Bragg reflection plus a monotonic background intensity due to random displacements. The second sum contains the Laue monotonic diffuse scattering[18] at $p=q$ case and periodic diffuse scatterings due to chemical short range ordering. This term can be reformed into a Fourier cosine series.

The second term in eq. (1) also gives periodic diffuse scatterings which consist of the summation of Fourier sine series[18].

The third term gives symmetric and antisymmetric diffuse scatterings in the vicinity of each Bragg reflection. Diffuse scattering observed between Bragg reflections are derived from (chemical) short-range correlations. On the other hand, the long range correlation, *e.g.* the strain field which is surrounding the microdomains, causes diffuse scattering in the vicinity of Bragg reflections.

III. Experimentals

A spherical $TaD_{0.55}$ sample with a diameter of 7 mmϕ was prepared from a 99.9% Ta single crystal made by the electron beam floating zone method. Deuterium gas was loaded at temperatures in a range from 300 to 600°C. The $TaD_{0.55}$ sample is a coarse grain multidomain crystal at room temperature but becomes a single crystal above the $\beta_1-\alpha$ phase transformation temperature at 54°C. The mosaic spread of the α-$TaD_{0.55}$ sample that was measured by the neutron beam by the ω-scan mode was about 0.25 degree, indicating a relatively good crystal. Temperature-dependent variation in the neutron diffraction intensities at the superlattice positions 001 and 110 (1/2 1/2 0 and 1/2 1/2 0 in the bcc lattice) of the orthorhombic β_1-phase indicated that the present sample directly transformed from a β_1-phase to a cubic α-phase. Figure 1 shows superlattice reflection intensities at 001 and 110 as a function of temperature. It is evident that the $\beta_1-\alpha$ phase transformation is typically of the first order.

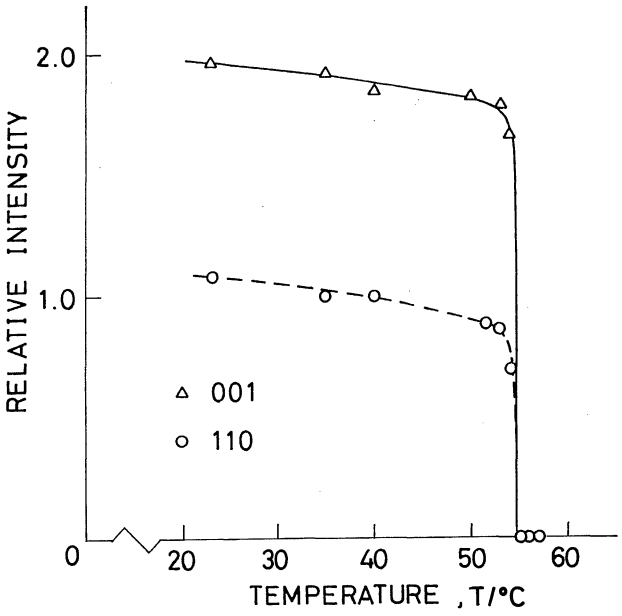

Fig. 1 Variation of 001 and 110 superlattice reflections of β_1-$TaD_{0.55}$. 001 and 110 reflections correspond to 1/2 1/2 0 and 1/2 1/2 1 reflections in the α-phase(bcc), respectively. β_1-α transformation occurs at 54°C.

The neutron diffraction work was conducted with the use of an automated 4-circle neutron diffractometer KID in a double axes configuration and a triple-axes neutron spectrometer CTNS in JRR-2 reactor hall in JAERI. For the measurement of pseudo-Bragg reflections, the KID diffractometer was used with the incident neutron beam monochromatized by a pyrolytic graphite at $\lambda=0.1$ nm. The collimation was kept at 40′-hole-30′ throughout the experiment. The diffuse scatterings in the vicinity of fundamental reflections were measured by the use of a triple-axes-neutron spectrometer (CTNS) with the incident neutron at $\lambda=0.14$ nm and the collimation of 30′-30′-30′-40′. The thermal diffuse scatterings (TDS) in the vicinity of fundamental reflections were effectively eliminated by the use of an analyzer crystal.

Temperature of the sample was regulated with a stability of ±0.3°C.

IV. Results

1. Pseudo-Bragg reflections

Figure 2 (a) and (b) show the diffraction intensity curves obtained along the hh0 and hh2 lines in the

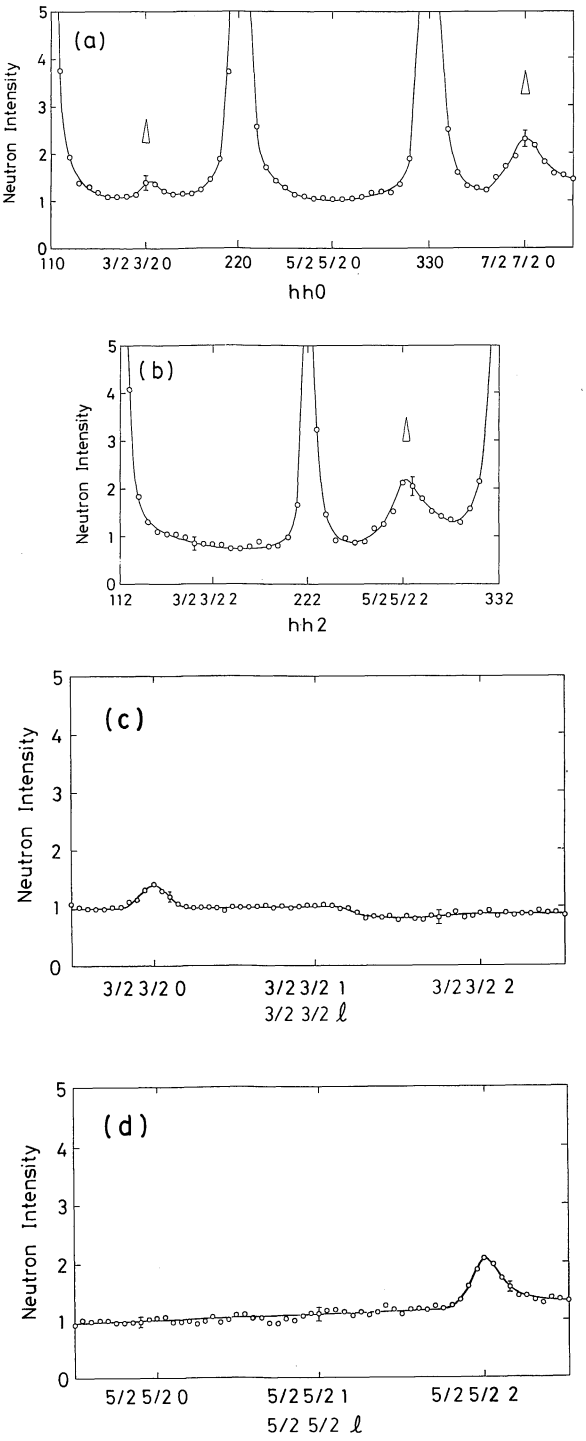

Fig. 2 (a) Diffuse scattering intensities on the hh0 line in α-$TaD_{0.55}$ at 65°C. Each point was counted for 30 min. Triangles indicate the instrumental resolution. (b) Diffuse scattering intensities on the hh2. (c) Diffuse scattering intensities on the 3/2 3/2 l line. The level change near the 3/2 3/2 1.3 is due to the incident neutron flux level change. See the diffuse pseudo-Bragg reflection at 3/2 3/2 1 is absent. (d) Diffuse scattering intensities on the 5/2 5/2 l line. Strong 5/2 5/2 2 pseudo-Bragg reflection is seen.

reciprocal lattice. There are 1/2 1/2 0 type diffuse reflections. Intensities of the diffuse reflections seemingly change in an alternative manner on the hh0 and hh2 lines. Strong diffuse scattering was observed in relatively higher wave number regions. 1/2 1/2 0 and its equivalent points correspond to superlattice reflections in the β_1- and β_2-$TaD_{0.48}$[19].

Figure 2 (c) and (d) show the diffraction intensity curves along the ⟨001⟩ direction. It looks significant that 1/2 1/2 1 type diffuse-reflections are absent in the present case. But these type diffuse reflections were observed in α-$VD_{0.78}$ by Sugizaki[20] and in α-NbD_x ($0.70<x<0.85$) by Shasnov *et al.*[7] The back ground level change in the Fig. 2(c) was due to the output level change of the reactor JRR-2 during the experiment.

Present authers[19] previously found that 1/2 1/2 1 type superlattice reflections are eliminated by the $\beta_1-\beta_2$ phase transformation in $TaD_{0.48}$ while 1/2 1/2 0 type reflections are retained. The crystal structures of the β_1- and β_2-phases are shown in Fig. 3. During the transformation, disordering of deuterium atoms occurs in the (001) deuterium planes, which are parallel to the (110) bcc planes.

It might be assumed that the diffuse pseudo-Bragg reflections in the present system is due to the microdomains having an ordered structure of the β_2-phase type.

The domain size estimated from the FWHM of diffuse pseudo-Bragg reflection at 7/2 7/2 0 point becomes 1.5–2.0 nm in both ⟨110⟩ and ⟨001⟩ directions.

Figure 4 shows temperature dependent variation of the 7/2 7/2 0 pseudo Bragg reflection. Although the intensity of the peak moderately reduced with increasing temperature from 65 to 80°C, the FWHM of the peak was kept at almost the same level, indicating that the total number of the microdomains is temperature dependent but the size of the domains is not much temperature sensitive.

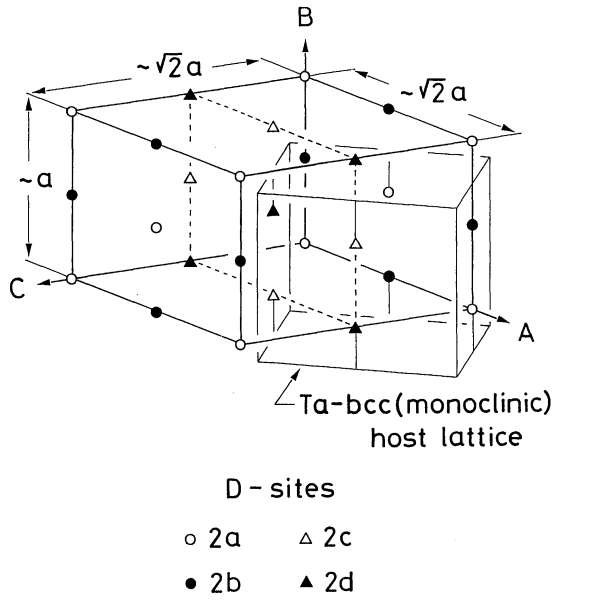

Fig. 3 Structure model of C222 (No. 21) β_1- and β_2-$TaD_{0.5}$. Solid lines indicate a unit cell. Thin lines indicate a tantalum sub-cell which is bcc in the α-phase. In the β_1-phase, only 2a sites are occupied, 2a and 2b sites are almost equally occupied in the β_2-phase.

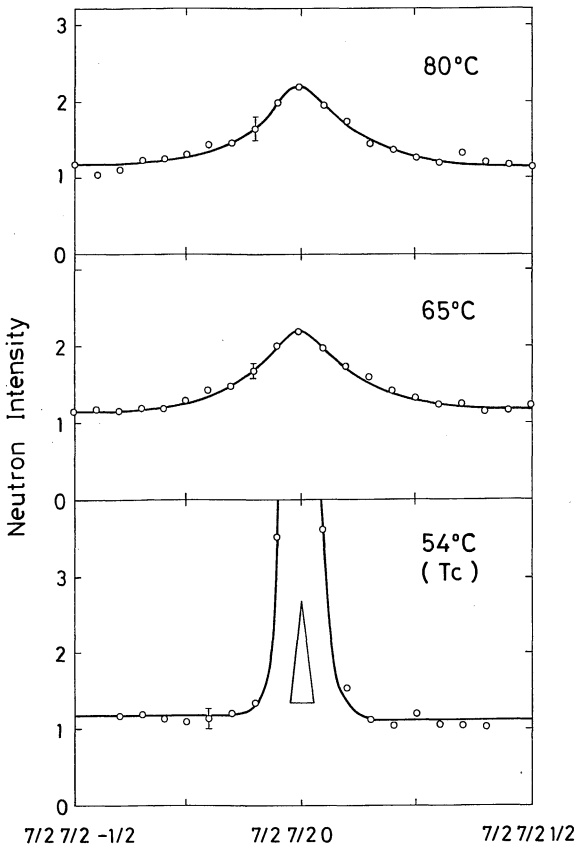

Fig. 4 Variation of scattering intensity distributions at 7/2 7/2 0 with increase of temperature from 54 to 80°C. The intensity of diffuse pseudo-Bragg reflection is not much temperature dependent. The FWHM is also retained during the temperature change from 65 to 80°C.

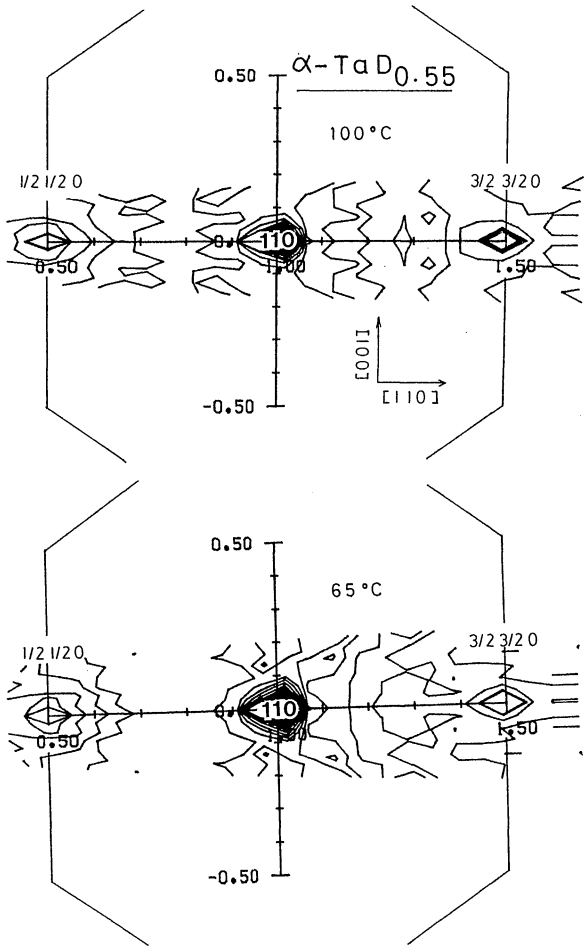

Fig. 5 Variation of diffuse scattering intensities in the vicinities of 110 point on (110) plane obtained by the use of a triple axes neutron spectrometer. Radially extended component and asymmetric wing component are seen. Diffuse intensities at 1/2 1/2 0 and 3/2 3/2 0 points are also seen. Sharp reflections at 1/2 1/2 0 and 3/2 3/2 0 are due to the contamination of $\lambda/2$-component in the incident beam. Thin lines in the figure indicate the Brillouin zone boundaries.

2. Huang and Trinkaus scattering

Temperature-dependent diffuse scatterings are observed in the vicinities of Bragg reflections. Figure 5 shows equi-intensity contour maps of diffuse scatterings in the vicinity of 110 at 65 and 100°C in the (110) plane. The diffuse intensities are evidently extended in the radial directions from the 000 reciprocal lattice point. Asymmetrical two wings are also seen near the vertical axis. Radially extended diffuse intensities, i.e. Huang scattering, indicate that microdomains which introduce hydrostatic distortion are embedded[8] in the matrix. Symmetrical nature in the radial component along [110] indicates that hydrostaic distortion in the vicinity of the particles decays slowly. On the other hand, the wing components are Trinkaus scattering[8][16] i.e. a kind of local-stress-induced scattering due to particles which give non-hydrostatic distortions. The asymmetric nature of the wing component indicates that the non-hydrostatic distortion, tetragonal or orthorhombic distortion in the present case, varies rather quickly in the vicinity of the particles or within the particles. The Trinkaus scattering decreases with increasing temperature form 65 to 100°C, corresponding with the depopulation of the microdomains.

The existence of hydrostatic and non-hydrostatic distortions in the matrix does not necessarily mean that there are two different kinds of microdomains embedded in the matrix. It is possible to assume that the non-hydrostatic distortion in the vicinity of the particles may change smoothly to a hydrostatic distortion in the matrix remote from the microdomains.

V. Discussion

Warren-Cowley's short-range order-parameter α_{pq} is calculated from the diffuse pseudo-Bragg reflections. Diffuse scattering in the vicinity of the Bragg reflections which are mainly due to the third term of eq. (1) are not taken into account to avoid the complexity.

Diffuse monotonic background intensities were subtracted. Then the diffuse scattering intensities are divided into the symmetric (cosine series) and antisymmetric (sine series) components. The former, corresponds to the chemical short range order term, and the latter to the

short range displacement term, respectively. The chemical short-range order term is derived from the atomic arrangements of interstitial deuterium atoms and vacant interstitial sites. On the other hand, the short range displacement term is derived from the displacements of tantalum atoms and interstitial deuterium atoms.

Figure 6 schematically shows the separation of diffuse scattering intensities. The separation was proceeded on the following assumptions.

(1) The chemical ordering term and the displacement term are perfectly cancelled at the wave number of 5/2 5/2 0 where no diffuse scattering was observed by the neutron diffraction.

(2) The intensity distribution due to the chemical ordering term is spherically symmetric in the vicinities of 1/2 1/2 0 and its equivalent wave numbers in the reciprocal lattice.

(3) The origin of the diffuse scattering is the presence of microdomains which have an ordered structure of β_2-$TaD_{0.5}$ type. The microdomains are enoughly separated. Otherwise, antiphase boundaries between the domains may cause fine structures[21] on the diffuse intensity distributions.

The displacement of interstitial deuterium site is prohibited by the symmetry of the β_2-$TaD_{0.5}$ type ordered structure. Possible displacement of tantalum atoms is $\langle z^{DTa} \rangle$ which is the displacement along the c-axis of the β_2-$TaD_{0.5}$ type structure.

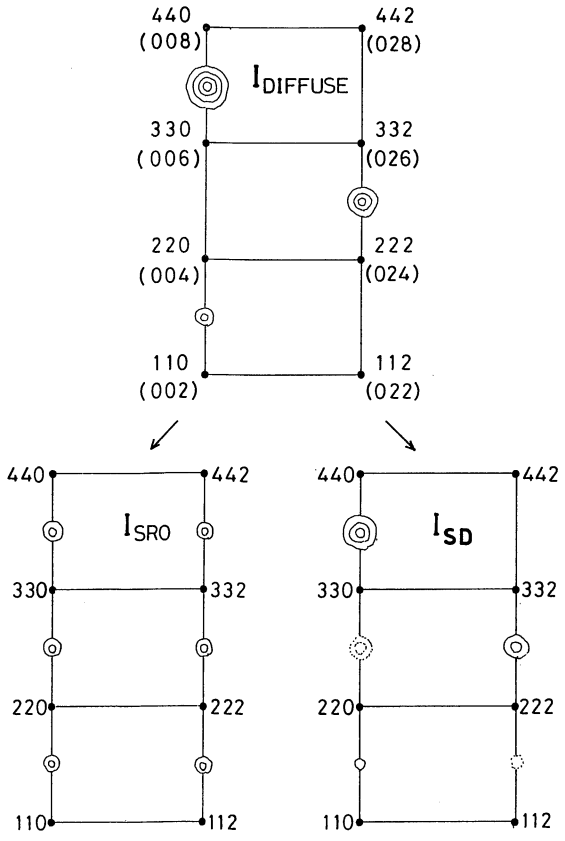

Fig. 6 Schematic diagram of the separation of diffuse intensities. I_{SRO} and I_{SD} are the intensities due to the chemical short range order and short range displacements, respectively.

Tables 1 and 2 are the calculated values of the short range order parameter and the displacement of metal atoms. The coordinates of atom sites were indexed referring to the β_2-$TaD_{0.5}$ unit cell. The order parameter in the perfectly ordered structures of β_1- and β_2-phases are also listed in Table 1. The order parameter is normalized so as to become 1.0 at the 000 position. Magnitude of the displacement, $\langle z^{DTa} \rangle$, are normalized by the normalization constant used for the chemical short range order term.

Figures 7 and 8 show the variation of the short range order parameter as a function of distance in the (001) and (100) planes of a β_2-phase microdomain, respectively. In both planes, the absolute values of the order parameter starts at the value 0.02 and vanishes in the distance more than 1.2 nm from the center. It implies that the β_2-phase domain is spherical or close to spherical with a diameter no more than 2.4 nm. The FWHM of the order parameter vs distance curve i.e. about 1.2 nm may be a good measure for the domain size.

Figure 9 shows an equi-α contour map on the (110) plane which is constructed from obtained short range order parameters shown in Table 1. There are practically three deuterium filled layers in a domain.

The strain tensor in the vicinity of the β_2-phase-like

Table 1 Calculated short range order parameter α_{lmn}.

Coordinates of D-atoms			α_{lmn}	β_1-phase	β_2-phase
l	m	n			
0	0	0	1.0	1.0	1.0
0	1/2	0	0.0206	−0.379	0.312
1/2	0	0	0.0195	−0.379	0.312
0	0	0	−0.0195	−0.379	−0.379
1/2	1/2	0	0.0185	1.0	0.312
0	1/2	1/2	−0.0185	−0.379	−0.379
0	1	0	0.0176	1.0	0.312
1/2	0	1/2	−0.0176	−0.379	−0.379
1/2	1/2	1/2	−0.166	−0.379	−0.379
1/2	1	0	0.0158	−0.379	0.312
0	1	1/2	−0.0158	−0.379	−0.379
1	0	0	0.0141	1.0	0.312
0	0	1	0.0141	1.0	0.312
1/2	1	1/2	−0.0141	−0.379	−0.379
1	1/2	0	0.0134	−0.379	0.312
0	1/2	1	0.0134	−0.379	0.312
0	3/2	0	0.0134	−0.379	0.312
1	0	1/2	−0.0126	−0.379	−0.379
1/2	0	1	0.0126	−0.379	0.312
1	1/2	1/2	−0.0120	−0.379	−0.379
1/2	1/2	1	0.0120	1.0	0.312
1/2	3/2	0	0.0120	1.0	0.312
0	3/2	1/2	−0.0120	−0.379	−0.379
1	1	0	0.0113	1.0	0.312
0	1	1	0.0113	1.0	0.312
0	2	0	0.0089	1.0	0.312
1/2	3/2	1/2	−0.0107	−0.379	−0.379
1	1	1/2	−0.0101	−0.379	−0.379
1/2	1	1	0.0101	−0.379	0.312
1	0	1	0.0090	1.0	0.312
1	3/2	0	0.0084	−0.379	0.312
0	3/2	1	0.0084	−0.379	0.312
1	1/2	1	0.0084	−0.379	0.312

Table 2 Calculated short range displacement $\langle z^{DTa} \rangle$ of tantalum atoms.

Coordinates of Ta-atms l	m	n	Displacement of Ta ($\times 10^{-3}$ nm)	Distance from 0 0 0 point (nm)
1/4	1/4	1/4	0.20	0.1889
1/4	3/4	1/4	0.17	0.3047
3/4	1/4	1/4	0.15	0.3872
1/4	1/4	3/4	−0.15	0.3872
3/4	3/4	1/4	0.13	0.4550
1/4	3/4	3/4	−0.13	0.4550
1/4	5/4	1/4	0.13	0.4550
3/4	1/4	3/4	−0.11	0.5140
3/4	5/4	1/4	0.10	0.5668
3/4	3/4	3/4	−0.10	0.5668
1/4	5/4	3/4	−0.10	0.5668
5/4	1/4	1/4	0.09	0.6152
1/4	1/4	5/4	0.09	0.6152
1/4	7/4	1/4	0.09	0.6152
5/4	3/4	1/4	0.08	0.6600
1/4	3/4	5/4	0.08	0.6600
3/4	5/4	3/4	−0.08	0.6600
5/4	1/4	3/4	−0.07	0.7020
3/4	1/4	5/4	0.07	0.7020
3/4	7/4	1/4	0.07	0.7020
1/4	7/4	3/4	−0.07	0.7020
5/4	5/4	1/4	0.06	0.7415
1/4	5/4	5/4	0.06	0.7415
5/4	3/4	3/4	−0.06	0.7415
3/4	3/4	5/4	0.06	0.7415
3/4	7/4	3/4	−0.05	0.7791
1/4	9/4	1/4	0.05	0.7791
5/4	5/4	3/4	−0.05	0.8149
3/4	5/4	5/4	0.05	0.8149
7/4	1/4	1/4	0.04	0.8492
1/4	1/4	7/4	−0.04	0.8492
5/4	7/4	1/4	0.04	0.8492
1/4	7/4	5/4	0.04	0.8492

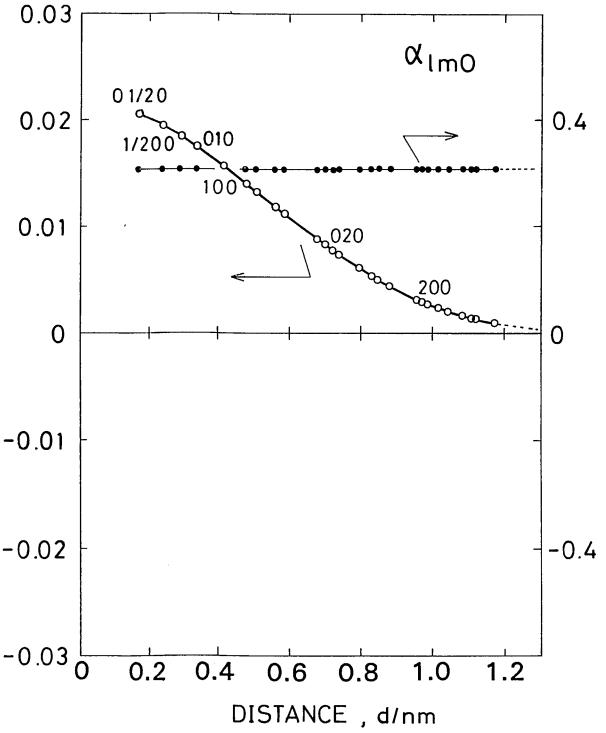

Fig. 7 Calculated short range order parameter α_{lmn} in the (001) plane as a function of distance.

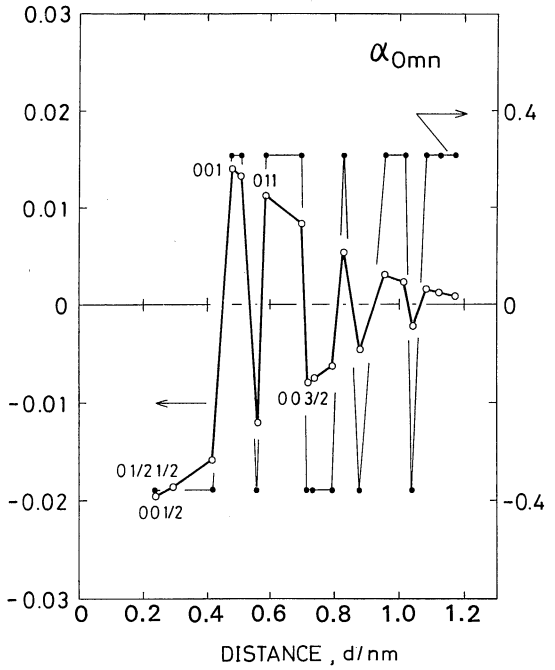

Fig. 8 Calculated short range order parameter in the (100) plane.

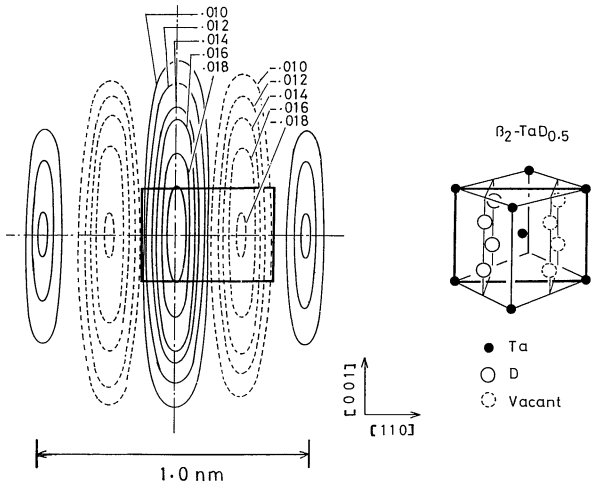

Fig. 9 Equi-α contour map in a real space. (110) cross section is represented. A rectangular drawn with thin lines corresponds to a (110) cross section of a bcc unit cell.

microdomain is almost the same as the $\alpha \rightarrow \beta_2$ transformation strain such as;

$$\varepsilon_{ij} = \begin{pmatrix} -2.98 & 4.52 & 0 \\ 4.52 & -2.98 & 0 \\ 0 & 0 & 4.07 \end{pmatrix} \times 10^{-3} \qquad (3)$$

which is calculated from the lattice parameters of α- and β_2-$TaD_{0.48}$[19]. Since the volume change is relatively small $\varepsilon_{11}+\varepsilon_{22}+\varepsilon_{33} = -1.89 \times 10^{-3}$, the stress induced diffuse scattering in the vicinity of fundamental reflections must be highly the Trinkaus-type, consistent with the present experimental results.

It is interesting to point out that the short range order

parameters at 0 1/2 0 and 1/2 0 0 sites in the β_2-phase are almost 7% of those in the β_2-phase. There are two structural models conceivably suitable to explain such low number. Many β_2-phase precipitate-like regions, that are the microdomains, may exist in the disordered matrix (model 1) or the sample is divided into domains which are small, about 2.4 nm in size, and have one of the six equivalent atomic arrangements of the β_2-phase (model 2). Relatively low short range order parameters at 0 1/2 0 and 1/2 0 0 sites can be explained in terms of the density of the β_2-phase precipitate-like microdomains (model 1) or in terms of the frequency of antiphase boundaries situated between the domains (model 2). Unfortunately, there is no direct experimental evidence to determine which microdomain-model is correct. Further experimental study is needed in this line. X-ray and neutron small-angle diffraction studies on the present sample are on the way. The results will be reported separately in near future.

VI. Conclusion

The short range order parameter α_{lmn} and the displacement parameter of Ta atoms are determined in the α-$TaD_{0.55}$ at 65°C from neutron diffuse scattering intensities. A microdomain-model considered to be reasonable from the experiment was adapted for the calculation. The domain shape, about 1.2 nm is nearly spherical. This value agrees well with the value, 1.5–2.0 nm, estimated from the FWHM of the 7/2 7/2 0 pseudo-Bragg reflection. Diffuse scatterings in the vicinity of Bragg reflections are explained by a microdomain-model.

Acknowledgment

The authors are grateful to Mr. K. Nemoto for the technical assistance with the neutron diffraction experiment. This work was partly supported by the Grant-in-Aid for the Scientific Research from the Ministry of Education, Science and Culture.

REFERENCES

(1) T. B. Douglas: J. Chem. Phys., **40** (1964,) 2248.
(2) W. A. Oates, J. A. Lambert and P. T. Gallagher: Trans. Met. Soc. AIME, **245** (1969) 47.
(3) V. A. Somenkov and S. Sh. Shill'stein: Z. Phys. Chem. (Neue Folge), **117** (1979), 125.
(4) H. S. U. Jo and S. C. Moss: Solid State Comm., **30** (1979), 365.
(5) E. Burkel, H. Behr, H. Metzger and J. Peisl: Phys. Rev. Lett., **46** (1981), 1078.
(6) T. O. Brun, S. M. Shapiro and H. K. Birnbaum: unpublished (1978).
(7) R. Shasnov: Ph. D. Thesis, University of Illinois, USA (1983); R. Shasnov, H. K. Birnbaum and S. M. Shapiro; Phys. Rev., **B33** (1986), 1732.
(8) P. H. Dederichs: J. Phys., **F3** (1973), 471.
(9) A. Magerl, J. J. Rush and J. M. Rowe: Phys. Rev., **B33** (1986), 2093.
(10) K. Watanabe and Y. Fukai: J. Phys. Soc. Japan, **54** (1985), 3415.
(11) B. Borie and C. J. Sparks: Acta Crystall., **17** (1964), 827.
(12) B. Borie and C. J. Sparks: ibid., **A27** (1971), 198.
(13) B. E. Warren, B. L. Averbach and B. W. Roberts: J. Appl. Phys., **22** (1951), 1493.
(14) B. Borie: Acta Crystall., **14** (1961), 472.
(15) K. Huang: Proc. Roy. Soc., **A190** (1947), 102.
(16) H. Trinkaus: Phys. Status Solidi, (b) **51** (1972), 307.
(17) J. W. Cowley: J. Appl. Phys., **21** (1944), 24.
(18) B. Borie: Acta Crystall., **10** (1957), 89.
(19) H. Kaneko, T. Kajitani and M. Hirabayashi: J. Less-Common Metals, **103** (1984), 45.
(20) Y. Sugizaki: Ph. D. Thesis, Tohoku University, Japan (1986).
(21) S. Hashimoto: Acta Crystall., **A30**, (1974), 792.